annalen der physik
www.ann-phys.org

Cosmological Parameters from Planck Data in $SU(2)_{CMB}$, Their Local ΛCDM Values, and the Modified Photon Boltzmann Equation

Ralf Hofmann, Janning Meinert,* and Shyam Sunder Balaji*

A review of the spatially flat cosmological model $SU(2)_{CMB}$, minimally induced by the postulate that the cosmic microwave background (CMB) is subject to an SU(2) rather than a U(1) gauge principle, is given. Cosmological parameter values, which are determined from the Planck CMB power spectra at small angular scales, are compared to their values in spatially flat ΛCDM from both local and global extractions. As a global model $SU(2)_{CMB}$ leans toward local ΛCDM cosmology and is in tension with some global ΛCDM parameter values. Spectral antiscreening / screening effects in $SU(2)_{CMB}$ radiance are presented within the Rayleigh– Jeans regime in dependence on temperature and frequency. Such radiance anomalies can cause CMB large-angle anomalies. Therefore, it is pointed out how $SU(2)_{CMB}$ modifies the Boltzmann equation for the perturbations of the photon phase space distribution at low redshift and why this requires to the solve the ℓ-hierarchy on a comoving momentum grid (q-grid) for all z.

1. Introduction

Our present age witnesses a promising change in paradigm on how to model and analyze the composition and dynamics of the Cosmos. This shift apparently is concerned with a departure from perturbative towards nonperturbative approaches.

Within flat ΛCDM one example on the modeling side is that nonlinear clustering observables (e.g., the galaxy-halo connection model) on cosmologically small comoving length scales (a few to tens of h^{-1}Mpc), which evolve out of adiabatic, Gaussian initial perturbations, not only are addressed by mild multiplicative deformations of their perturbatively evolved versions[1] but by nonperturbative, high-resolution N-body simulations.[2,3] In contrast to the former the latter method does not require anchoring in high-z observables, which rely on a specific cosmological model, is valid if scales are not too small[3] and exhibits large signal-to-noise ratios in weak lensing signals.[2]

An example on the theoretical side is deconfining SU(2) Yang– Mills thermodynamics with an a priori estimate of the thermal ground state based on self dual, topologically nontrivial gauge-field configurations.[4] Relying on this result and on direct observation at low frequencies,[5] a postulate on the CMB being subject to an SU(2) rather than a U(1) gauge principle can be made, henceforth referred to as $SU(2)_{CMB}$. The Yang– Mills scale (or critical temperature T_c for the deconfining–preconfining transition[6]) of this model is fixed by CMB radio-frequency observations.[5,7]

The flat ΛCDM model is a minimal and successful framework to accommodate a wealth of cosmological data.[8–11] Throughout the last decade, however, tensions were uncovered in certain parameter values of this model when determined by data referring to local versus global cosmology, see Abdalla et al.,[12] for a recent comprehensive review. Most profoundly, there is the Hubble crisis. This is expressed by aan up to $\approx 5\sigma$ discrepancy between the value $H_0 \approx 73.5\text{km s}^{-1}\text{ Mpc}^{-1}$ (errors ranging between 1 and 2.5 km s^{-1} Mpc^{-1}) as extracted from the Hubble diagram in local, flat ΛCDM, see for example, Riess et al.,[13] using calibrated standard candles, or from strong-lensing time delays (cosmography, only astrophysics model dependence), see Wong et al.,[14] and $H_0 \approx (67.27 \pm 0.60)\text{km s}^{-1}\text{ Mpc}^{-1}$ fitted to CMB two-point power spectra by the Planck collaboration[15] with similarly low values obtained from BAO (standard ruler) data[10] assuming flat ΛCDM to be valid globally. Next, global fits of flat ΛCDM and BBN yield a baryon density which is by a factor $\approx 3/2$ higher than the value observed by direct baryon census, see for example, Aghanim et al.,[15] Kirkman et al.,[16] Shull et al.,[17] Johnson et al.,[18] for the latter claim. Moreover, within flat ΛCDM weak gravitational lensing effects persistently indicate a value of the clustering amplitude,[2,19,20] which relates to a value of σ_8, being by 2–3 σ lower compared to the value extracted from CMB

R. Hofmann, J. Meinert, S. S. Balaji
Institut für Theoretische Physik
Universität Heidelberg Philosophenweg 12
D-69120 Heidelberg, Germany
E-mail: R.Hofmann@ThPhys.Uni-Heidelberg.de;
J.Meinert@ThPhys.Uni-Heidelberg.DE

J. Meinert
Department of Physics
Bergische Universität Wuppertal
Gaußstraße 20, D-42119 Wuppertal, Germany

The ORCID identification number(s) for the author(s) of this article can be found under https://doi.org/10.1002/andp.202200517

DOI: 10.1002/andp.202200517

observation.[15,21] Also, there is a mild tendency for an increase of Ω_m (by a maximum significance of $\approx 1\sigma$ in Miyatake et al.[2]) compared to the CMB extraction in Aghanim et al.[15] Finally, we point out a $\approx 2\sigma$ tension in the redshift z_{re} for reionization between direct observation using the Gunn– Peterson trough.[22] and the latest extraction from the Planck data.[15]

In addition to these anomalies in flat ΛCDM parameter values, there are large-angle anomalies in the CMB, hinting at a dynamical breaking of statistical isotropy relevant to these angular scales.[23–26] These anomalies can be distinguished as follows: lack of large-angle CMB temperature correlation, hemispherical power asymmetry, octopole planarity and alignment with the quadrupole, point-parity anomaly, variation in cosmological parameters over the sky, and cold spot. For a comprehensive, very recent summary see Abdalla et al.[12]

The purpose of the present paper is twofold. In the first half, we explain the cosmological model implied by $SU(2)_{CMB}$ and its present status in fitting it to Planck data in Hahn et al.,[27] in particular focusing on the dark-sector parametrization and a physical realization thereof proposed in Meinert and Hofmann.[28] Flat ΛCDM emerges at low redshifts in this model, and we compare the according parameter values with those of recent weak-lensing and galaxy clustering analyses, local Hubble-diagram fits, observations of the onset of the epoch of reionization by the detection of the Gunn–Peterson trough in the spectra of distant quasars, and direct baryon censuses. This is confronted with the extraction of flat ΛCDM parameters in global cosmology probes (CMB and BAO). As a result, we see a tendency that Ω_m is increased and σ_8 decreased compared to these global fits. In particular, the latest results on weak-lensing galaxy– galaxy correlation using the HSC Y1 and SDSS data yield central values of these two parameters coinciding with those of the model in Hahn et al.,[27] albeit the significance of Ω_m's deviation only is 1σ. Moreover, the model in Hahn et al.[27] obtains values of other cosmological parameters which point toward the values extracted from local probes. Most noticeably the value of $H_0 \approx (74.24 \pm 1.46)$,km s^{-1} Mpc^{-1} deviates by less than 1σ from that of Riess et al.[13] The latter, in turn, deviates from global extractions in flat ΛCDM by more than 5σ. At the moment, we interpret this as an encouragement to further pursue $SU(2)_{CMB}$ but by no means as a confirmation. In particular, the goodness of the CMB fits to TT, TE, and EE of Hahn et al.[27] may be questioned, even at high ℓ, although the errors of associated parameters are comparable to those obtained from ΛCDM fits.

In the second half of the paper, we revisit the modification of the conventional Planck spectrum of blackbody radiance at low frequencies and temperatures with the intention to eventually implement this spectral anomaly into a particular CMB Boltzmann solver—CLASS.[29–31] We hope[26,32,33] that proper implementation of the according comoving energy–momentum relation in such a code conveys some of the above mentioned large-angle anomalies[23,25] even though the projection onto C_ℓ's assumes statistical isotropy. Presently, we face technical problems in the implementation, however. This concerns the introduction of a grid in comoving momentum q for the photon Boltzmann hierarchy. Therefore, no results on the low-ℓ CMB angular power spectra are presented here.[34,35] Hoping that experts in the CMB modeling community can be interested in overcoming these problems in a reasonable amount of time, desirably in collaboration with the present authors, we provide the required comoving photon dispersion law in $SU(2)_{CMB}$.

This paper is organized as follows. In Section 2 we review the minimal, spatially flat cosmological model $SU(2)_{CMB}$, as it was employed in Hahn et al.[27] in fits to 2015 Planck data. We also discuss dark-sector physics, based on ultralight Planck-scale axion species,[28] which the minimal dark sector of $SU(2)_{CMB}$ in Hahn et al.[27] may be mimicking. Cosmological parameter values extracted in Hahn et al.[27] are compared with global and recent local extractions within flat ΛCDM or by cosmography to point out a tendency of $SU(2)_{CMB}$ as a global model leaning toward local, flat ΛCDM. Section 3 first provides a brief review of large-angle anomalies in the CMB, based on analyses of the two satellite missions WMAP and Planck. The radiatively induced antiscreening/screening effects in the Rayleigh– Jeans regime, which are described by the screening function G for the thermal $SU(2)_{CMB}$ photon, could explain the CMB large-angle anomalies, see Ludescher and Hofmann,[33] Hofmann.[26] Therefore, we review this blackbody anomaly of spectral radiance both as a function of temperature and frequency. As a so far not discussed aspect, we point out that the maximal deviation between U(1) and $SU(2)_{CMB}$ radiances is constantly feeble at temperatures considerably larger than $T_c = T_0 = 2.725$ K, rendering its detection at high temperatures, say $T = 300$, K, experimentally challenging. Next, we discuss the effects of screening function G on the Boltzmann equation for the cosmological evolution of linear perturbations of photon phase-space distribution in conformal Newtonian gauge. Since low-redshift (low-z) photons suffer antiscreening/screening a nontrivial comoving energy–momentum relation persists, exhibiting a dependence on conformal time τ. Moreover, a match between high-z and low-z evolution needs to be made when solving the Boltzmann hierarchy on a comoving momentum grid (q-grid) for *all* τ, including active Thomson scattering. Finally, we point out which modules of the Boltzmann code CLASS are affected by the modified cosmological model $SU(2)_{CMB}$ to simultaneously address the CMB power spectra at high-ℓ for cosmological parameter extraction and at low-ℓ to mitigate the discrepancy of TT power seen in Hahn et al.[27] Such a lowering of TT power would be a smoking gun for the breaking of statistical isotropy at low redshift mediated by $SU(2)_{CMB}$.

2. Present Status of $SU(2)_{CMB}$

2.1. T–z Relation and Other Implications for the Cosmological Model

The change due to $SU(2)_{CMB}$ in spatially flat FLRW cosmology, which, as a background model, appreciably starts deforming ΛCDM at redshifts well within the dark ages, is induced by a modified CMB temperature (T) - redshift (z) relation (TRR). In the literature, the CMB TRR was reported to be extracted from two probes: i) the thermal Sunyaev– Zel'dovich effect (thSZ)[36,37] using an X-ray hot cluster of galaxies as a probe, or ii) absorber clouds with atomic/ionic/molecular transitions (finestructure, rotation levels) in the lines of sight of background sources (quasars, bright galaxies).[38] Method (i) was applied at low redshifts for example, in Hurier et al.,[39] method (ii) at higher redshifts in Molaro et al.,[40] Noterdaeme et al.,[41,42] Songaila et al.,[43] Ge et al.,[44] Srianand et al.,[45] Muller et al.,[46] and Riechers

et al.[47] with a Milky-Way validation in Roth et al.,[48] Mather et al.[49]

In both methods (i) and (ii) a frequency-redshift relation (FRR) $\nu' = (1+z)\nu(z=0)$ is used to relate observed frequency $\nu(z=0)$ to the frequency ν' that associates with the transition in the CMB probe studied. It can easily be shown that the use of a TRR with $T(z) = f(z)T(z=0)$ and an FRR with $\nu' = g(z)\nu(z=0)$, in spite of predicting the usual redshift relation of the Stefan– Boltzmann law, is inconsistent[50] with a CMB blackbody spectrum at $z > 0$ if $f(z) \neq g(z)$. Therefore, if the CMB is assumed to be a blackbody for $z > 0$, which is the basis for (i) and (ii), both methods are bound to generate the TRR $T(z) = (1+z)T(z=0)$ because of the use of the FRR $\nu' = (1+z)\nu(z=0)$, see Hofmann[51] for more details.

For the reader's convenience we repeat here the arguments put forward in Hahn et al.[27] how the modified TRR comes about in $SU(2)_{CMB}$ and what it implies.

In an (energy conserving) FLRW universe one demands

$$\frac{d\rho_{YM}}{da} = -\frac{3}{a}\left(\rho_{YM} + P_{YM}\right) \tag{1}$$

where ρ_{YM} and P_{YM} denote energy density and pressure, respectively, in the deconfining phase of SU(2) Yang– Mills thermodynamic, and a refers to the cosmological scale factor, normalized to $a(T_0) = 1$, where $T_c = T_0 = 2.725$ K indicates the present baseline temperature of the CMB,[52] interpreted as the critical temperature T_c for the deconfining-preconfining phase transition in Hofmann.[7] The solution of Equation(1) can be recast as

$$a \equiv \frac{1}{z+1} = \exp\left(-\frac{1}{3}\log\left(\frac{s_{YM}(T)}{s_{YM}(T_0)}\right)\right) \tag{2}$$

Here the entropy density s_{YM} is given as

$$s_{YM} \equiv \frac{\rho_{YM} + P_{YM}}{T} \tag{3}$$

which shows that the a priori estimates of the thermal ground-state contributions to pressure and energy density do not contribute to Equation (2). For large temperatures, $T \gg T_0$, Equation (2) can be simplified[53] as

$$\frac{T(z)}{T_0} = (1/4)^{1/3}(z+1) \approx 0.63\,(z+1) \tag{4}$$

The number 1/4 is the ratio between the number n_p of relativistic degrees of freedom in constituting the gauge-field excitations of the plasma at T_0 ($n_p = 2$) and for $T \gg T_0$ ($n_p = 8$). For temperatures T not much higher than T_0 linearity in the T–z relation is violated by the Yang– Mills scale Λ (related to T_0 by $\Lambda = 2\pi T_0/13.87$[4]) breaking conformal invariance. Therefore, we define the multiplicative deviation $\mathcal{S}(z)$ from linear scaling at any given temperature T in the deconfining phase as

$$\mathcal{S}(z) = \left(\frac{\rho_{YM}(z=0) + P_{YM}(z=0)}{\rho_{YM}(z) + P_{YM}(z)}\,\frac{T^4(z)}{T_0^4}\right)^{1/3} \tag{5}$$

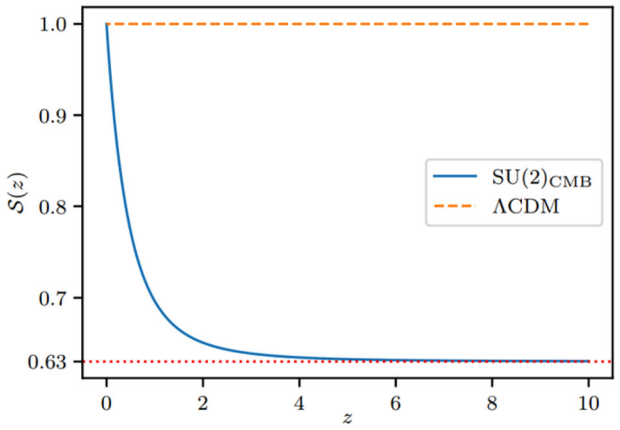

Figure 1. Plot of function $\mathcal{S}(z)$ of Equation (5), defined as a (multiplicative) deviation from the linear T–z relation of Equation (4). The curvature in $\mathcal{S}(z)$ at low z indicates the breaking of conformal invariance in the deconfining SU(2) Yang– Mills plasma for $T \approx T_0$ with a rapid approach toward $(1/4)^{1/3} \approx 0.63$ as z increases. Adapted with permission.[28] Copyright 2019, Oxford U Press.

As a result, the T–z relation assumes the generally valid form

$$\frac{T(z)}{T_0} = \mathcal{S}(z)\,(z+1) \quad (T \geq T_0) \tag{6}$$

Figure 1 depicts function $\mathcal{S}(z)$.

For the conformally invariant Yang–Mills gas and for $T \gg T_0$, when all eight gauge modes are nearly massless,[54] the z dependence of the deconfining Yang—Mills energy density ρ_{ym} is implied by Equation (4) to be

$$\rho_{YM}(z) = 4\left(\frac{1}{4}\right)^{4/3}\rho_\gamma(z) = \left(\frac{1}{4}\right)^{1/3}\rho_\gamma(z) \quad (z \gg 1) \tag{7}$$

Here, ρ_γ denotes the energy density of a thermal photon gas, using the U(1) T–z relation $T = T_0(z+1)$. Again, for low temperatures conformal invariance is broken, and Equation (7) needs to be modified accordingly, see Hahn et al.[27] For the z dependence of the energy density of massless neutrinos one has for $T \gg T_0$

$$\Omega_\nu(z) = \frac{7}{8}N_{eff}\left(\frac{16}{23}\right)^{4/3}\Omega_{YM,\gamma}(z) \tag{8}$$

In Equation (8) a modified factor for the conversion of neutrino to CMB temperature occurs because of additional relativistic degrees of freedom during e^+e^- annihilation,[55] $\Omega_{YM,\gamma}(z)$ refers to the photon part of the density parameter in deconfining $SU(2)_{CMB}$ thermodynamics (screening/antiscreening effects, off-Cartan fluctuations, and thermal ground-state contribution excluded), and N_{eff} is the effective number of massless neutrino flavors. As in Hahn et al.[27] we set N_{eff} equal to its 2015 Planck value:[56] $N_{eff} = 3.046$.

The postulate $SU(2)_{CMB}$ affects the comoving sound horizon $r_s(z)$, whose value at recombination (baryon drag) is the anchoring scale for the analysis of large-scale structure based on BAO, not only via the Hubble parameter $H(z)$ but also via the sound velocity c_s of the baryon-Yang–Mills plasma conventionally

modeled in terms of baryons interacting via photons. In general, $r_s(z)$ is given as

$$r_s(z) \equiv \int_z^\infty \mathrm{d}z' \, \frac{c_s(z')}{H(z')} \tag{9}$$

where the sound velocity is represented by

$$c_s(z) \equiv \frac{1}{\sqrt{3(1+R(z))}} \tag{10}$$

In what follows the subscript l refers to the quantity computed in ΛCDM. Specifically, the ratio R_l relates to entropy densities s_l or energy densities ρ_l of baryons (b) and photons (γ) as

$$R_l \equiv \frac{s_{l,\mathrm{b}}(z)}{s_{l,\gamma}(z)} = \frac{3}{4}\frac{\rho_{l,\mathrm{b}}(z)}{\rho_{l,\gamma}(z)} \quad (z \gg 1) \tag{11}$$

The generalization of Equation (11) to the baryon-Yang–Mills plasma replaces $s_{l,\gamma}(z)$ or $\rho_{l,\gamma}(z)$ by $s_{ym}(z)$ or $\rho_{\mathrm{YM},\gamma}(z)$, respectively, and $s_{l,\mathrm{b}}$ or $\rho_{l,\mathrm{b}}(z)$ by $s_{ym,\mathrm{b}}$ or $\rho_{ym,\mathrm{b}}(z)$, respectively, to define $R_{\mathrm{YM},\gamma}$, see Hahn et al.[27]

For the epoch of recombination the postulate $\mathrm{SU(2)_{CMB}}$ predicts a significantly higher redshift than ΛCDM does. Namely, equating the temperature of both models at $T \gg T_0$, using Equation (4) for $\mathrm{SU(2)_{CMB}}$ and $T/T_0 = z+1$ for ΛCDM, we arrive at

$$z_l = \left(\frac{1}{4}\right)^{1/3} z_{\mathrm{YM},\gamma} \tag{12}$$

In particular, this yields

$$z_{ym,\mathrm{rec}} = 1730 \tag{13}$$

based on $z_{l,\mathrm{rec}} = 1090$.[14,56] Repeating the argument of Hahn et al.,[27] we now infer from Equation (13) a dramatic reduction of the matter density parameter $\Omega_{\mathrm{YM},\gamma,m,0}$ during the epoch of recombination in $\mathrm{SU(2)_{CMB}}$ compared to ΛCDM. For this purpose it is entirely sufficient to describe recombination in terms of thermodynamics (Saha approximation). The Thomson scattering rate Γ then is a function of the recombination temperature T_{rec} only: $\Gamma = \Gamma(T_{\mathrm{rec}})$. Note that T_{rec} is independent of any cosmological model as long as thermodynamics prevails. Moreover, the Hubble parameter H depends on T_{rec} via z_{rec}: $H(z_{\mathrm{rec}}) = H(z(T_{\mathrm{rec}}))$. The additional assumption, that H is matter dominated during recombination turns out to be selfconsistent, see Hahn et al.[27] Eliminating Γ from the decoupling conditions in both models, $H_{\mathrm{YM},\gamma}(z_{ym,\mathrm{rec}}) = \Gamma(T_{\mathrm{rec}}) = H_l(z_{l,\mathrm{rec}})$, we thus conclude that

$$\Omega_{l,m,0} \approx 4\,\Omega_{\mathrm{YM},\gamma,m,0} \tag{14}$$

The most economic way for the modified cosmological model to simultaneously obey the postulate $\mathrm{SU(2)_{CMB}}$ globally and mimick ΛCDM at low redshifts[57] is the instantaneous emergence of dark matter (edm) from dark energy at some redshift $z_p < z_{\mathrm{YM},\gamma,\mathrm{rec}}$. From now on we set $z \equiv z_{\mathrm{YM},\gamma}$. Therefore, the following density parameter for the dark sector (ds) was proposed in Hahn et al.[27]

$$\Omega_{\mathrm{ds}}(z) = \Omega_\Lambda + \Omega_{\mathrm{pdm},0}(z+1)^3 + \Omega_{\mathrm{edm},0} \begin{cases} (z+1)^3, & (z < z_p) \\ (z_p+1)^3, & (z \geq z_p) \end{cases} \tag{15}$$

In Equation (15) today's density parameters for dark energy and dark matter are denoted by Ω_Λ and $\Omega_{\mathrm{pdm},0} + \Omega_{\mathrm{edm},0} \equiv \Omega_{\mathrm{cdm},0}$, respectively, $\Omega_{\mathrm{pdm},0}$ refers to primordial dark matter for all z, and $\Omega_{\mathrm{edm},0}$ associates with dark matter emergent from dark energy at z_p. In the following a brief discussion of the physics, potentially responsible for the dark-sector model in Equation (15), is given following ref. [28]. There the dark sector starts out at the Big Bang with four species of dark energy three of which have undergone transitions into dark matter in the past; one species yet is to face such a transition and therefore plays the role of a cosmological constant at present. The theoretical underpinning of such a dark-sector model is the invocation of the axial anomaly by SU(2) Yang–Mills theories, subject to a universal Planckian Peccei–Quinn scale.[58] Three out of four theories presently are in confining phases with their Yang–Mills scales relating to the masses of charged leptons. Such a link to particle physics is based on the assertion that lepton doublets are emergent phenomena in pure SU(2) Yang–Mills theories.[59,60] The associated axion particles receive their masses m_{a} via the axial anomaly[61–65] invoked by topological charges residing in the ground states of these Yang–Mills theories and are ultralight. With a universal Planckian Peccei– Quinn scale axion masses m_{a} thus scale like the squares of charged lepton masses m, for example, $m_{\mathrm{a},\mu}/m_{\mathrm{a,e}} = m_\mu^2/m_{\mathrm{e}}^2$.[28]

A depercolation transition from a homogeneous, superhorizon sized axion condensate (dark energy) toward a gas of nonrelativistic lumps (cold dark matter) of fuzzy dark matter (condensate core/soliton plus Navarro– Frenk– White halo)[66–70] occurs when the Hubble radius r_{H} matches the Bohr radius r_{B} modulo a phenomenologically determined, multiplicative constant $\alpha_e \approx 55\,500$, compare with Meinert and Hofmann.[28] For the axion particle associated with the electron this depercolation transition is parameterized in Equation (15) to occur at $z_{\mathrm{p}} = z_{\mathrm{p},e} = 53$. The two other depercolation transitions, associated with the muon and the tau, are found to occur at $z_{\mathrm{p},\mu} = 40\,000$ and $z_{\mathrm{p},\tau} = 685\,000$ in Meinert and Hofmann,[28] respectively. Because the Hubble radius at τ-lump depercolation is $r_{\mathrm{H}}(z_{p,\tau} = 685\,000) \approx 1.36 \times 10^{-6}$,Mpc this corresponds to a lower comoving cutoff scale of 0.93 Mpc for the linear density contrast generated by adiabatic curvature perturbations. For μ-lump depercolation we have $r_{\mathrm{H}}(z_{\mathrm{p},\mu} = 40\,000) \approx 3.74 \times 10^{-4}$Mpc, corresponding to a comoving cutoff scale of 14.94 Mpc. These two cutoff scales are well inside the nonlinear regime.[2] For e-lump depercolation $r_{\mathrm{H}}(z_{\mathrm{p},e} = 53) \approx 16.48$ Mpc is obtained, associated with a comoving cutoff scale of 873 Mpc. Therefore, the assumption made in Meinert and Hofmann[28] that density perturbations in the e-lump gas are triggered by those of the τ-lump and μ-lump gases is consistent for comoving scales up to 873 Mpc. Beyond this scale e-lump density perturbations are seeded by adiabatic curvature perturbations upon their horizon entry.

2.2. Cosmological Parameters: $\mathrm{SU(2)_{CMB}}$ versus Local and Global Observations in ΛCDM

The spatially flat, global cosmological model, minimally implied by $\mathrm{SU(2)_{CMB}}$ as outlined in Section 2.1, and flat ΛCDM, considered as a globally valid cosmological model, produce the parameter values in the table below (**Table 1**) when fitted to 2015 Planck

Table 1. Best-fit cosmological parameters of flat $SU(2)_{CMB}$ to the data in Ade et al.[56] (first column) as well as flat ΛCDM model to the data in Ade et al.,[56] employing the TT, TE, EE + low P + lensing likelihoods (second column) and to the data in Aghanim et al.,[71] employing the TT, TE, EE + low E + lensing likelihoods (third column). For $SU(2)_{CMB}$ the HiLLiPOP + low TEB + lensing likelihood is used as defined in Aghanim et al.[71] (low P and low TEB are pixel-based likelihoods). The upper section of the table quotes free parameter values, the lower section states the values of derived parameters. Errors correspond to 68% confidence levels.

Parameter	$SU(2)_{CMB}$	ΛCDM (2015)	ΛCDM (2018)
$\omega_{b,0}$	0.0173 ± 0.0002	0.02226 ± 0.00016	0.02237 ± 0.00015
$\omega_{pdm,0}$	0.113 ± 0.002	–	–
$\omega_{edm,0}$	0.0771 ± 0.0012	–	–
$100\,\theta_*$	1.0418 ± 0.0022	1.0408 ± 0.00032	1.04092 ± 0.00031
τ_{re}	0.02632 ± 0.00218	0.063 ± 0.014	0.0544 ± 0.0073
$\ln(10^{10} A_s)$	2.858 ± 0.009	3.059 ± 0.025	3.044 ± 0.014
n_s	0.7261 ± 0.0058	0.9653 ± 0.0048	0.9649 ± 0.0042
z_p	52.88 ± 4.06	–	–
H_0/km s^{-1}Mpc^{-1}	74.24 ± 1.46	67.51 ± 0.64	67.36 ± 0.54
z_{re}	$6.23^{+0.41}_{-0.42}$	$8.5^{+1.4}_{-1.2}$	7.67 ± 0.73
z_*	1715.19 ± 0.19	1090.00 ± 0.29	1089.92 ± 0.25
z_d	1640.87 ± 0.27	1059.62 ± 0.31	1059.94 ± 0.30
$\omega_{cdm,0}$	0.1901 ± 0.0023	0.1193 ± 0.0014	0.1200 ± 0.0012
Ω_Λ	0.616 ± 0.006	0.6879 ± 0.0087	0.6847 ± 0.0073
$\Omega_{m,0}$	0.384 ± 0.006	0.3121 ± 0.0087	0.3153 ± 0.0073
σ_8	0.709 ± 0.020	0.8150 ± 0.0087	0.8111 ± 0.0060
$S_8 \equiv \sigma_8 \sqrt{\Omega_{m,0}/0.3}$	0.802 ± 0.029	0.8313 ± 0.0176	0.8315 ± 0.0137
Age/Gyr	11.91 ± 0.10	13.807 ± 0.026	13.797 ± 0.023

data,[27] for the corresponding TT power spectrum see Appendix A. For completeness we also quote the values of flat ΛCDM fitted to 2018 Planck data.[15]

As the table indicates, there are statistically significant deviations between flat $SU(2)_{CMB}$ and flat ΛCDM, most noticeably in H_0. This $\approx 4.6 - 4.7\sigma$ discrepancy is comparable to the one extracted from the Hubble diagram in *local* flat ΛCDM, see for example, Riess et al.,[13] using calibrated standard candles, or from strong-lensing time delays (cosmography, only astrophysics model dependent extraction of H_0), see Wong et al.[14] On the other hand, fits of flat ΛCDM to BAO (standard ruler) and 2015 Planck data[10] yield a value of H_0 which is close to the fit of flat ΛCDM to the 2015 and 2018 Planck data alone: (67.6 ± 0.5) km s^{-1}Mpc^{-1} versus (67.51 ± 0.64) km s^{-1}Mpc^{-1} (Planck 2015) and (67.36 ± 0.54) km s^{-1}Mpc^{-1} (Planck 2018), respectively. All cosmological parameters are $\approx 1\sigma$ consistent in flat ΛCDM (2015) and flat ΛCDM (2018). It should be mentioned though that the high (low)-ℓ χ^2 per d.o.f. with $\ell \geq 30$ ($2 \leq \ell < 30$) is about 6% (1.5%) larger in flat $SU(2)_{CMB}$ than in flat ΛCDM fitted to the 2015 Planck data. This suggests that the present implementation of the flat $SU(2)_{CMB}$ within an FLRW cosmological model or this model for thermal photon gases itself has difficulties. The second option could be addressed by a dedicated terrestrial search for the blackbody spectral anomaly first derived in Schwarz et al.[72] and re-addressed in Section 3.2.1.

Let us now discuss baryon density $\omega_{b,0}$. Global fits of flat ΛCDM to the Planck data and BBN yield a baryon density which is by about a factor ≈3/2 higher than the value observed by direct, local census, see for example, refs. [15, 16, 56] for the former and refs. [17, 18] for the latter claim. The significance of this deviation is about 2σ. The same tendency of such a discrepant value of $\omega_{b,0}$ is seen in the table when comparing flat $SU(2)_{CMB}$ and flat ΛCDM, albeit at a higher significance.

Next, in ΛCDM weak gravitational lensing effects persistently indicate a value of the clustering amplitude[2,19,20] characterized by $\sigma_8 = 0.718^{+0.044}_{-0.031}$ in Miyatake et al.,[2] which is by 2–3σ lower compared to its value extracted from CMB observation, see table and refs. [15, 56]. As the table indicates, in $SU(2)_{CMB}$ the same tendency occurs, subject to a higher significance of 5.3 σ. Also, there is a mild tendency for an increase of Ω_m in local observations (by a maximum significance of $\approx 1\sigma$ in Miyatake et al.[2]) compared to the CMB extraction in Ade et al.,[56] and Aghanim et al.[15] Such a tendency is also seen in the table, albeit now with a significance of 7.5 σ.

Finally, there is a $\approx 2\sigma$ tension in the redshift z_{re} for reionization between direct observation using the Gunn– Peterson trough Becker et al.[22] and extraction of $z_{re} = 7.67 \pm 0.73$ from the 2018 Planck data.[15] For the 2015 Planck data, $z_{re} = 8.5^{+1.4}_{-1.2}$ this tension is again at $\approx 2\sigma$. From the table we see that the tension between flat $SU(2)_{CMB}$ and flat ΛCDM is 1.6σ (2015 Planck data) and 2σ (2018 Planck data).

It is conspicuous that the *global* flat model $SU(2)_{CMB}$ yields key cosmological parameter values which agree better with those of *local* flat ΛCDM extractions rather than those of *global* flat ΛCDM fitted to the same Planck data. Notice the unusually low value of the spectral index n_s of adiabative curvature perturbations in $SU(2)_{CMB}$, indicating a red-tilted spectrum. This may turn out to be an artefact of velocity divergence being suppressed on smaller scales due to late-time axion-condensate depercolation (e-lumps) but a modeling of the transition through an instantaneous transmission of this perturbation from the primordial gas (μ-lumps and τ-lumps), see Hahn et al.[27] That is, in reality the primordial spectrum may well be scale invariant but is fitted to be red-tilted due to missing velocity divergence on smaller scales. To gain more confidence in such an interpretation a thorough modeling of the depercolation transition in the framework of fuzzy dark matter (Poisson– Schrödinger system) is required, see for example, Schive et al.[69]

3. CMB at Large Angles

3.1. Observational Situation

As exhibited in Section 2.2, the global cosmological model flat ΛCDM deviates in some key parameter values from both local flat ΛCDM and the global flat model $SU(2)_{CMB}$ (fitted to Planck data and determined by angular scales associated with $l > 50$[12,27]). In addition, there are inadequacies at large angular scales, see, for example Hinshaw et al.,[73] Tegmark et al.,[23] and Copi et al.,[74,75] for missing power in the TT correlation on angular scales larger than 60° and the breaking of statistical isotropy expressed by low-ℓ multipole alignment in the map of CMB temperature fluctuations.[24–26,76] More specifically, based on the analysis of the two satellite missions WMAP and Planck, CMB large-angle anomalies fall into one of the following categories: lack of large-angle CMB temperature correlation (sketched above),

hemispherical (dipolar) power and variance asymmetries, for example. Eriksen et al.,[77] Ade et al.,[56] and Akrami et al.,[78] octopole planarity and alignment with the quadrupole, for example, de Oliveira-Costa et al.,[79] Copi et al.,[80] Notari and Quartin,[81] Schwarz et al.,[82] point-parity anomaly, for example, Kim and Naselsky,[83] Aluri and Jain,[84] and Gruppuso et al.,[85] variation in cosmological parameters over the sky, for example, Fosalba and Gaztañ aga,[86] Yeung and Chu,[87] and cold spot, for example, Vielva et al.,[88] Cruz et al.,[89] and Akrami et al.[78]

There are many attempts at explaining the CMB large-angle anomalies in the literature, ranging from a nontrivial topology of the Universe over an unusually large matter void invoking the integrated Sachs– Wolfe effect to features in the spectra of initial perturbations, see Abdalla et al.[12] for a recent compilation of these proposals. Here instead we focus on a dynamical, late-time breaking of statistical isotropy which peaks at redshift $z \approx 1$ and is induced by screened/antiscreened photon propagation in the framework of $SU(2)_{CMB}$ Hofmann.[26] This effect is expected to reduce the low-ℓ excess in the TT power spectrum of Hahn and Hofmann,[90] see Appendix A.

3.2. Modified $SU(2)_{CMB}$ Dispersion Law and CMB Boltzmann Solvers

3.2.1. Modified Photon Radiance in $SU(2)_{CMB}$

As explained in Schwarz et al.,[72] and Hofmann,[91] the modified black-body spectral intensity $I_{SU(2)}(\nu)$ of the SU(2) theory is obtained from that of the conventional U(1) theory as follows

$$I_{SU(2)}(\nu) = I_{U(1)}(\nu) \times \left(1 - \frac{G(\nu)}{\nu^2}\right) \theta\left(\nu - \nu^*\right) \tag{16}$$

where the characteristic cutoff-frequency ν^* is defined implicitly through

$$|\vec{p}|(\nu^*) = \sqrt{(2\pi\nu^*)^2 - G} = 0 \tag{17}$$

and $\theta(x)$ denotes the Heaviside function. It was shown in Falquez et al.[92] that

$$\nu^*(T) \propto T^{-1/2}, \quad (T \gg T_c) \tag{18}$$

In SI units one has

$$I_{U(1)}(\nu) \equiv \frac{2h}{c^2}\, \nu^3\, n_B\left(\frac{h\,\nu}{k_B\, T}\right) \tag{19}$$

where k_B is Boltzmann's constant, h is Planck's quantum of action, c denotes the speed of light in vacuum, and $n_B(x) \equiv 1/(e^x - 1)$. For the massless mode propagating into the spatial 3-direction, $\vec{p}||e_3$, and resorting back to natural units, $c = k_B = \hbar = 1$, the screening function $G(\nu)$ is computed in cylindrical coordinates and reads[93]

$$\frac{G}{T^2} = \int d\xi \int d\rho\, e^2 \lambda^{-3} \left(-4 + \frac{\rho^2}{4e^2}\right) \rho\, \frac{n_B\left(2\pi\lambda^{-3/2}\sqrt{\rho^2 + \xi^2 + 4e^2}\right)}{\sqrt{\rho^2 + \xi^2 + 4e^2}} \tag{20}$$

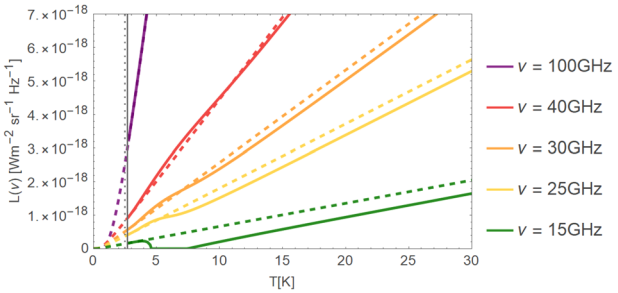

Figure 2. SU(2) Yang– Mills thermodynamics exhibits three phases:[4] the confining phase below $T_H \approx 0.9\,T_c$ (the Hagedorn temperature T_H indicated by the vertical gray dotted line), the preconfining phase for $T_H \leq T \leq T_c$ (T_c indicated by the vertical gray line), and the deconfining phase for $T \geq T_c$. In $SU(2)_{CMB}$ one has $T_c = T_0 = 2.725$K. SI units of radiance $L(\nu)$ are W m^{-2} sr^{-1} Hz^{-1}. The U(1) Rayleigh– Jeans radiances are given in dashed lines for $\nu = 15$GHz (green), 25 GHz (yellow), 30 GHz (orange), 40 GHz (red), and 100 GHz (purple) while solid lines depict the associated radiances in $SU(2)_{CMB}$.

where $\lambda \equiv 13.87\, T/T_c$ (T_c the critical temperature for the deconfining-preconfining phase transition), and e denotes the effective gauge coupling $e \geq \sqrt{8\pi}$. The support of the integration in Equation (20) is determined from the demand that ρ and ξ satisfy one or both of the two following conditions

$$\left|\frac{G}{T^2}\frac{\lambda^3}{(2\pi)^2} \pm \frac{\lambda^{3/2}}{\pi}\left(\sqrt{X^2 + \frac{G}{T^2}}\sqrt{\rho^2 + \xi^2 + 4e^2} - X\xi\right) + 4e^2\right| \leq 1 \tag{21}$$

where $X = X(T,\nu) \equiv |\vec{p}|/T = \sqrt{(2\pi\nu)^2 - G}/T$. For the SU(2) radiance one obtains.[92]

$$L_{SU(2)}(T,\nu) = L_{U(1)} \times \left(1 - \frac{G}{(2\pi\nu)^2}\right) \theta\left(\nu - \nu^*\right) \tag{22}$$

and specifically for $SU(2)_{CMB}$ one has $T_c = T_0 = 2.725$,K.[5,7] In **Figure 2** the temperature dependence of spectral black-body radiance in the range from 0–30 K is shown for five different frequencies in case of $SU(2)_{CMB}$ and the conventional U(1) theory. Notice the gap at the lowest frequency of 15 GHz and the shifted linear dependence (pseudo Rayleigh– Jeans) to the right of this gap due to screening in $SU(2)_{CMB}$. With increasing frequencies there is antiscreening at low temperature, which transitions into screening at higher temperatures. Both temperature regimes, screening and antiscreening, approach the U(1) radiance rapidly as frequency increases. **Figure 3** depicts the frequency dependence of spectral black-body radiance from 0 to 50 GHz for three different temperatures. It can be seen from the spectra that the deviation $\Delta L(\nu) \equiv |L_{U(1)}(\nu) - L_{SU(2)_{CMB}}(\nu)|$ is maximal at $\nu = \nu^*$ where $\Delta L(\nu) = L_{U(1)}(\nu)$. This is true for all temperatures. Since $L_{U(1)}(\nu) \propto \nu^2\, T$ in the Rayleigh– Jeans regime and using Equation (18), we conclude that

$$\Delta L(\nu^*) = 4.85 \times 10^{-19}\,\mathrm{W\,m^{-2}\,sr^{-1}\,Hz^{-1}}, \quad (T \gg T_c) \tag{23}$$

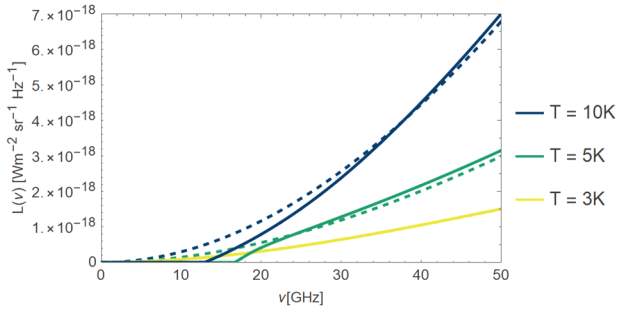

Figure 3. The $SU(2)_{CMB}$ and the U(1) black-body spectral radiances are shown for $T = 3$K (yellow), 5 K (green) and 10 K (blue) in solid and dashed lines, respectively. The spectral gap is widest at $\approx 2 \times T_c \approx 5$,K. The spectral regime, where U(1) radiance is larger/smaller than $SU(2)_{CMB}$ radiance, exhibits screening/antiscreening.

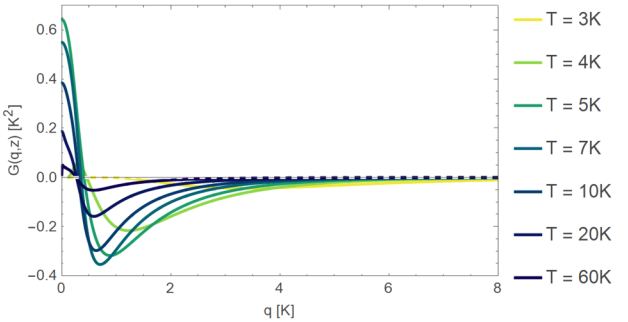

Figure 4. Screening function $G(q, z)$ as a function of comoving momentum modulus q and for the following temperature/redshift values: 3 K (z=0.29, yellow), 4 K (z=1.16, light green), 5 K (z=1.85, green), 7 K (z=3.07, petrol), 10 K (z=4.83, blue), 20 K (z=10.66, dark blue), and 60 K (z=33.96, darkest blue). The white-dashed line depicts the U(1) situation $G \equiv 0$.

and in particular at room temperature. The feableness of such a small, maximal deviation between U(1) and $SU(2)_{CMB}$ radiances renders the detection of the spectral anomaly at temperatures $T \gg T_c$ an experimentally challenging task.

3.2.2. Boltzmann Equation for Linear Perturbations of Photon Phase-Space Distribution

The low-frequency, low-temperature modifications of the thermal photon dispersion law in $SU(2)_{CMB}$ discussed in Section 3.2.1 imply technical difficulties in the treatment of the Boltzmann hierarchy for the perturbations $F_\gamma(\vec{k}, \hat{n}, q, \tau)$ and $G_\gamma(\vec{k}, \hat{n}, q, \tau)$ of the photon phase-space distribution in CMB codes such as CLASS.[30,94] Here $\hat{n} \equiv \vec{q}/q$. These complications arise when evolving the latter, in comoving $\vec{k}$-space and at some comoving-momentum modulus q, through the low-z (or large-τ) regime.[29] More precisely, the low-z, collisionless Boltzmann equation needs to maintain the q-dependence in the perturbations $F_\gamma(\vec{k}, \hat{n}, q, \tau)$ and $G_\gamma(\vec{k}, \hat{n}, q, \tau)$ because the ratio q/ε (ε the comoving energy, see Equation (26) below) depends on conformal time τ. Here we define the perturbations (sum and difference of perturbations associated with the two independent linear polarization states) F_γ and G_γ through the perturbed phase-space distribution f as

$$f_\gamma(\vec{k}, \hat{n}, q, \tau) \equiv f_0(q) \left[1 + F_\gamma(\vec{k}, \hat{n}, q, \tau) + G_\gamma(\vec{k}, \hat{n}, q, \tau)\right] \tag{24}$$

where

$$f_0 = f_0(\varepsilon) = \frac{1}{4\pi^3} \frac{1}{e^{\varepsilon(q,a)/(S(z)T_0)} - 1} \tag{25}$$

In Equation (25) T_0 is today's CMB temperature, and a denotes the cosmological scale factor with $a(\tau_0) = 1$ where τ_0 refers to the present conformal time. In the case of thermalized photons in $SU(2)_{CMB}$, a modified comoving energy– momentum dispersion law applies[4,29,95] as

$$\varepsilon(q, a) = \sqrt{q^2 + a^2 G(q, a)} = \sqrt{q^2 + \frac{G(q, z)}{(z+1)^2}} = \varepsilon(q, z) \tag{26}$$

where G denotes the transverse screening function, discussed in Section 3.2.1 and given in Equations (20) and (21), but now understood as a function of comoving momentum modulus q and scale factor a (or redshift $z = 1/a - 1$) instead of X and T. We convert $\frac{G}{T^2}(X, T)$ of Equation (20) to $G(q, z)$ by appealing to $X = q(z+1)/T(z)$ and $T(z) / T_0 = S(z)(z+1)$, see Equation (6).

From **Figure 4** and Equation (26) we infer that for increasing z one rapidly runs into the regime of the U(1) dispersion law, $\varepsilon = q$. In particular, the U(1) dispersion law applies prior to and through recombination.

In conformal Newtonian gauge, the linear perturbation $\Psi(\vec{k}, \hat{n}, q, \tau) = F_\gamma(\vec{k}, \hat{n}, q, \tau) + G_\gamma(\vec{k}, \hat{n}, q, \tau)$ evolves according to the Boltzmann equation[29]

$$\frac{\partial \Psi}{\partial \tau} + i\frac{q}{\varepsilon}(\vec{k} \cdot \hat{n})\Psi + \frac{\mathrm{d} \ln f_0}{\mathrm{d} \ln q}\left[\dot{\phi} - i\frac{\varepsilon}{q}(\vec{k} \cdot \hat{n})\psi\right] = \frac{1}{f_0}\left(\frac{\partial f}{\partial \tau}\right)_C \tag{27}$$

where ϕ and ψ are the gravitational potentials, and the right-hand side is the collision term. This term is only relevant prior to and through recombination and depends on $F_\gamma(\vec{k}, \hat{n}, q, \tau)$ and $G_\gamma(\vec{k}, \hat{n}, q, \tau)$ separately.[29] The expansion of $F_\gamma(\vec{k}, \hat{n}, q, \tau)$ and $G_\gamma(\vec{k}, \hat{n}, q, \tau)$ into Legendre polynomials $P_\ell(\hat{k} \cdot \hat{n})$ (ℓ=0, 1, 2, ⋯) yields coefficients $F_{\gamma,\ell}(\vec{k}, q, \tau)$ and $G_{\gamma,\ell}(\vec{k}, q, \tau)$ which evolve in τ (or z) according to a Boltzmann hierarchy.[29] To perform a match of high-z and low-z (and therefore large-angle) downward evolutions at some appropriate, intermediate value z_{match} we notice that the need to retain the q-dependence in $F_{\gamma,\ell}(\vec{k}, q, \tau)$ and $G_{\gamma,\ell}(\vec{k}, q, \tau)$ at low z (not integrating it out) also requires to keep it at high z where antiscreening/screening effects of $SU(2)_{CMB}$ can safely be neglected. Therefore, the Boltzmann hierarchy needs to be solved on a q-grid for all z. In **Figure 5** the z-evolution of the factor q/ε, which induces this complication, is shown for low values of z.

3.2.3. Structure of CLASS

Having i) reviewed the main features of $SU(2)_{CMB}$ as a cosmological model, see Hahn et al.,[27] and ii) considered the CMB at large angular scales within deconfining SU(2) Yang– Mills thermodynamics, see Ludescher and Hofmann[33] and Hofmann,[26]

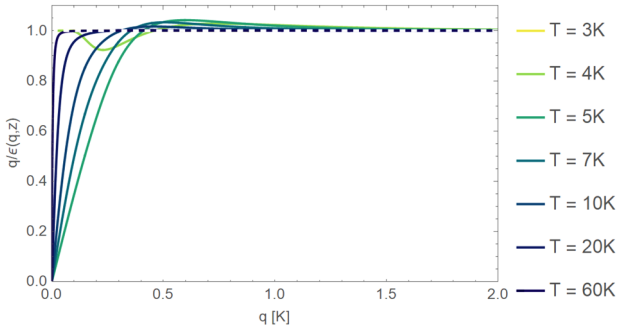

Figure 5. Shown is $q/\epsilon(q,z)$ as a function of comoving momentum q and for the following temperature/redshift values: 3 K ($z = 0.29$, yellow), 5 K ($z = 1.85$, green), 7 K ($z = 3.07$, petrol), 10 K ($z = 4.83$, blue), 20 K ($z = 10.66$, dark blue), and 60 K ($z = 33.96$, darkest blue). The U(1) behavior $q/\epsilon \equiv 1$ largely coincides with the behaviors at 3 and 60 K and is shown in terms of a white-dashed line.

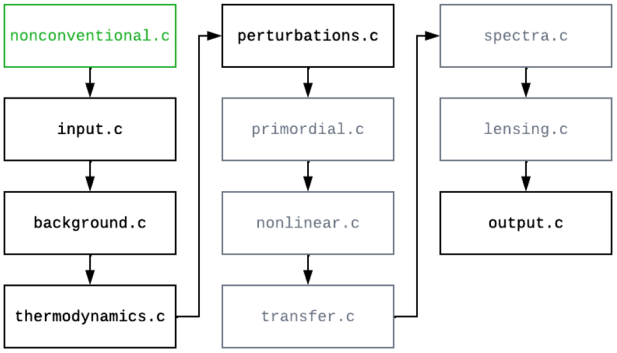

Figure 6. Modules of CLASS. The module *nonconventional.c* was introduced in Hahn et al.[27] into the backbone of CLASS. The modules in black contain $SU(2)_{CMB}$ modifications whereas the modules in gray are untouched.

we may now discuss what it takes to quantitatively confront $SU(2)_{CMB}$ with the observed large-angle anomalies discussed in Section 3.1.

Several CMB Boltzmann codes are available such as CMBFAST[96–98] and CLASS.[30] Here we choose to discuss CLASS due to its flexibility, speed, and good documentation which also has motivated its use in Hahn et al.[27]

CLASS is written in pure C and includes the following modules: *input.c, background.c, thermodynamics.c, perturbations.c, primordial.c, nonlinear.c, transfer.c, spectra.c, lensing.c,* and *output.c.* Each of these modules performs specific tasks and feed their outputs into the subsequent module along the aforementioned order. The following modifications were implemented in Hahn et al.:[27]

i) A module called *nonconventional.c* was added which computes the thermodynamical quantities ρ_{ym} (energy density), P_{ym} (pressure), and the scaling function $\mathcal{S}(z)$ of Equations (5) and (6) in $SU(2)_{CMB}$.
ii) The module *input.c* contains all input and precision parameters. Additional cosmological parameters in $SU(2)_{CMB}$ such as z_p, $\Omega_{\mathrm{edm},0}$ and the new conversion between the neutrino temperature T_ν and the CMB temperature T, see Equation (8), are introduced here.
iii) The module *background.c* solves the Friedmann equation and stores other quantities such as the energy densities of individual species (ρ_i), the critical density (ρ_c), the Hubble parameter H, and conformal time τ. Within this module, the new cosmological model is implemented according to Section 2.1. Also, the ratio $R_{ym} \equiv \frac{s_b(z)}{s_{ym}(z)} = \frac{3}{4}\frac{\rho_b(z)}{\rho_{ym}(z)}$, see Equation (11) and text following it, is defined here.
iv) The module *thermodynamics.c* evolves the baryon-photon plasma, relying on the modified sound speed $c_s(z) \equiv 1/(3(1 + R_{ym}(z)))$, and stores quantities such as the ionization fraction χ_e as well as recombination and reionization redshifts. The modified T–z relationship for $SU(2)_{CMB}$ in Equation (6) is implemented within this module.
v) The module *perturbations.c* solves the perturbations evolution for each specified particle species and gravity. This module also includes the Euler equation for the emergent dark matter component.[27]
vi) The *output.c* module is extended to include the new $SU(2)_{CMB}$ parameters.

All other modules, namely *primordial.c, nonlinear.c, transfer.c, spectra.c,* and *lensing.c* are not directly affected by $SU(2)_{CMB}$. **Figure 6** provides an overview on CLASS modules, how they depend on one another, and which modules are modified/added in Hahn et al.[27] due to $SU(2)_{CMB}$.

To address large-angle anomalies via a modification in the hierarchy for perturbations of the photon phase-space distribution, as discussed in Section 3.2.1, we foresee the following changes in the $SU(2)_{CMB}$ modified version of CLASS:

A) We are required to set up a function in *class.c* which calls the screening function $G(q, z(\tau))$ for a given comoving momentum q and redshift z (and thus conformal time τ) from precomputed tables.
B) In the *perturbations.c* module, the evolution of the perturbations of the photon phase-space distribution needs to be performed on a q-grid along an ℓ-hierarchy (similar to the non-cold dark matter species description in Lesgourgues and Tram[94]). This also requires the introduction of functions ϵ (Equation (26)) and q/ϵ as well as the corresponding modification of $\frac{d\ln f_0}{d\ln q}$ in Equation (27).

The bottleneck is the implementation of the q-grid in the Boltzmann hierarchy for $F_{\gamma,\ell}$ and $G_{\gamma,\ell}$ which also involves the collision terms that are active prior to and throughout recombination (high-z case). Moreover, a matching[99] at some intermediate z_{match} with $1 \ll z_{\mathrm{match}} \ll z_*$ of high-z and low-z evolutions needs to implemented in *perturbations.c* on the q-grid such that power spectra do not depend on the choice of z_{match}.

It is hoped that a group with good experience in the implementation of the hierarchy for massive neutrinos in CLASS may be interested in pursuing the above mentioned code modifications, desirably in collaboration with the present authors.

4. Summary and Outlook

In the present paper we have reviewed the cosmological model $SU(2)_{CMB}$ which assumes that the CMB is subject to deconfining SU(2) Yang– Mills thermodynamics and a spatially flat Universe. This model coincides with flat ΛCDM locally. However, due to a modified temperature (T)—redshift (z) relation $SU(2)_{CMB}$ deviates strongly from flat ΛCDM at high z with profound implications for the dark-sector physics. Cosmological parameter values, which are not affected by low-z physics or the low-ℓ multipoles, were extracted in Hahn et al.[27] by fits to 2015 Planck power spectra. The corresponding model then yields an excess of low-ℓ power in TT which we address in the second part of the present paper in terms of photon screening/antiscreening effects at low z. Here, we confirm that there is indeed no influence of these effects on cosmological parameter fitting. We have compared the according parameter values of $SU(2)_{CMB}$ with extractions from cosmologically local and global data within flat ΛCDM or within a cosmographic context. As a result, we see a tendency of $SU(2)_{CMB}$ as a global model to lean toward locally extracted cosmological parameter values of H_0, z_{re}, ω_b, σ_8, and Ω_m.

The low-z spectral radiance antiscreening/screening anomalies in the Rayleigh-Jeans regime of deconfining $SU(2)_{CMB}$ thermodynamics were not considered in Hahn et al.[27] but are expected to relate to the large-angle anomalies of the CMB[26,33] and to induce a lowering of low-ℓ power in TT, see Figure A1 in Appendix A. Their implementation in CMB Boltzmann codes is arduous because of the need to introduce a q-grid for the Boltzmann hierarchy of perturbations to the photon phase-space distribution and a match of low-z with high-z evolutions. Hoping that groups more experienced with the implementation of Boltzmann codes for massive, relativistic species may be interested in pursuing an $SU(2)_{CMB}$ code modification, desirably together with the present authors, we have provided information on the low-z dependence of the screening function G and the associated modified comoving energy-momentum relation for the photon. We have also discussed which CLASS modules need to be targeted in implementing $SU(2)_{CMB}$ modifications, both for the cosmological model[27] and the linear perturbations thereof.

If the $SU(2)_{CMB}$ modifications of CMB codes proposed in the present paper turn out to yield the lowering of low-ℓ power in TT under the assumption of statistical isotropy in projecting onto the C_ℓ's, this would motivate a dedicated analysis of statistical isotropy breaking in terms of less inclusive statistics as a next step. Also, as discussed in Section 2.2, a modeling of the depercolation transition from dark energy to dark matter, using the framework of fuzzy dark matter from ultralight axions, would refine Equation (15) and yield insights in nonlinear structure formation on small scales.[2]

Appendix A: $SU(2)_{CMB}$ CMB Fit

A lowering of the TT power spectrum for small ℓ is expected[26] when taking screening/antiscreening effects into account in the comoving dispersion law of the low-z photon, see Equation (26) and Figure 5. This may close the red shaded area in **Figure A1** below. Beyond such a lowering of small-ℓ TT power, the investigation of statistical-isotropy breaking, induced by a cosmologically local temperature depression and characterized by a typical gradient[24,26] requires less inclusive statistics, see for example, Schwarz et al.[82]

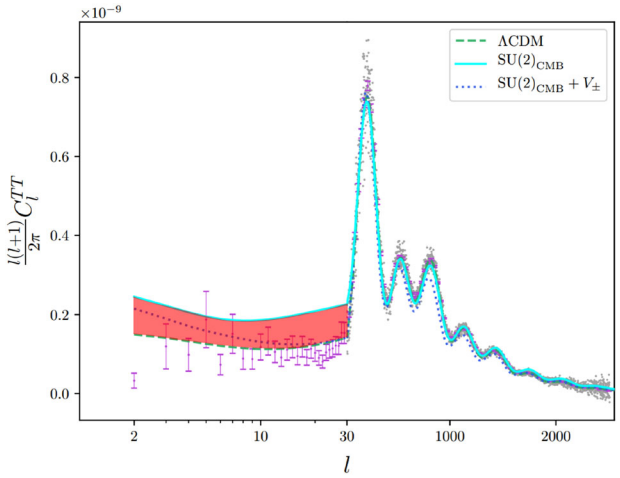

Figure A1. Normalized power spectra of TT correlator for best-fit parameter values quoted in Table 1. Adapted with permission.[27] Copyright 2019, Oxford U Press.

Acknowledgements

J.M.'s work was supported by the Vector Foundation under grant number P2021-0102. The authors would like to acknowledge useful discussions with Daniel Kramer and Philip Matthias.

Open access funding enabled and organized by Projekt DEAL.

Conflict of Interest

The authors declare no conflict of interest.

Data availability statement

The *Mathematica* notebooks for the computation of the screening function G and the coefficient q/ϵ as well as the modified CLASS code of Hahn et al.[27] are available from the authors upon request.

Keywords

cosmological model, deconfining SU(2) Yang– Mills thermodynamics, fuzzy dark matter, galactic structure, modified dark sector, thermal ground state, temperature-redshift relations

Received: October 27, 2022
Revised: February 11, 2023
Published online: May 16, 2023

[1] S. Sugiyama, M. Takada, H. Miyatake, T. Nishimichi, M. Shirasaki, Y. Kobayashi, S. More, R. Takahashi, K. Osato, M. Oguri, J. Coupon, C. Hikage, B.-C. Hsieh, Y. Komiyama, A. Leauthaud, X. Li, W. Luo, R. H. Lupton, H. Murayama, A. J. Nishizawa, Y. Park, P. A. Price, M. Simet, J. S. Speagle, M. A. Strauss, M. Tanaka, *arXiv:2111.10966*, **2021**.

[2] H. Miyatake, S. Sugiyama, M. Takada, T. Nishimichi, M. Shirasaki, Y. Kobayashi, R. Mandelbaum, S. More, M. Oguri, K. Osato, Y. Park, R. Takahashi, J. Coupon, C. Hikage, B.-C. Hsieh, A. Leauthaud, X. Li, W. Luo, R. H. Lupton, S. Miyazaki, H. Murayama, A. J. Nishizawa, P. A. Price, M. Simet, J. S. Speagle, M. A. Strauss, M. Tanaka, N. Yoshida, *arXiv:2111.02419*, **2021**.

[3] H. Miyatake, Y. Kobayashi, M. Takada, T. Nishimichi, M. Shirasaki, S. Sugiyama, R. Takahashi, K. Osato, S. More, Y. Park, *arXiv:2101.00113*, **2020**.
[4] R. Hofmann, *The Thermodynamics of Quantum Yang-Mills Theory: Theory and Applications*, 2nd ed., World Scientific, Singapore **2016**.
[5] D. J. Fixsen, A. Kogut, S. Levin, M. Limon, P. Lubin, P. Mirel, M. Seiffert, J. Singal, E. Wollack, T. Villela, C. A. Wuensche, *Astrophys. J.* **2011**, *734*, 5.
[6] R. Hofmann, *Entropy* **2016**, *18*, 310.
[7] R. Hofmann, *Ann. Phys.* **2009**, *18*, 634.
[8] A. G. Riess, A. V. Filippenko, P. Challis, A. Clocchiatti, A. Diercks, P. M. Garnavich, R. L. Gilliland, C. J. Hogan, S. Jha, R. P. Kirshner, B. Leibundgut, M. M. Phillips, D. Reiss, B. P. Schmidt, R. A. Schommer, R. Chris Smith, J. Spyromilio, C. Stubbs, N. B. Suntzeff, J. Tonry, *Astron. J.* **1998**, *116*, 1009.
[9] S. Perlmutter, G. Aldering, G. Goldhaber, R. A. Knop, P. Nugent, P. G. Castro, S. Deustua, S. Fabbro, A. Goobar, D. E. Groom, I. M. Hook, A. G. Kim, M. Y. Kim, J. C. Lee, N. J. Nunes, R. Pain, C. R. Pennypacker, R. Quimby, C. Lidman, R. S. Ellis, M. Irwin, R. G. McMahon, P. Ruiz-Lapuente, N. Walton, B. Schaefer, B. J. Boyle, A. V. Filippenko, T. Matheson, A. S. Fruchter, N. Panagia, et al., *Astrophys. J.* **1999**, *517*, 565.
[10] S. Alam, M. Ata, S. Bailey, F. Beutler, D. Bizyaev, J. A. Blazek, A. S. Bolton, J. R. Brownstein, A. Burden, C.-H. Chuang, J. Comparat, A. J. Cuesta, K. S. Dawson, D. J. Eisenstein, S. Escoffier, H. Gil-Marín, J. N. Grieb, N. Hand, S. Ho, K. Kinemuchi, D. Kirkby, F. Kitaura, E. Malanushenko, V. Malanushenko, C. Maraston, C. K. McBride, R. C. Nichol, M. D. Olmstead, D. Oravetz, N. Padmanabhan, et al., *Mon. Not. R. Astron. Soc.* **2017**, *470*, 2617.
[11] C. L. Bennett, M. Halpern, G. Hinshaw, N. Jarosik, A. Kogut, M. Limon, S. S. Meyer, L. Page, D. N. Spergel, G. S. Tucker, E. Wollack, E. L. Wright, C. Barnes, M. R. Greason, R. S. Hill, E. Komatsu, M. R. Nolta, N. Odegard, H. V. Peiris, L. Verde, J. L. Weiland, *Astrophys. J. Suppl.* **2003**, *148*, 1.
[12] E. Abdalla, G. F. Abellán, A. Aboubrahim, A. Agnello, O. Akarsu, Y. Akrami, G. Alestas, D. Aloni, L. Amendola, L. A. Anchordoqui, R. I. Anderson, N. Arendse, M. Asgari, M. Ballardini, V. Barger, S. Basilakos, R. C. Batista, E. S. Battistelli, R. Battye, M. Benetti, D. Benisty, A. Berlin, P. D. Bernardis, E. Berti, B. Bidenko, S. Birrer, J. P. Blakeslee, K. K. Boddy, C. R. Bom, A. Bonilla, et al., *arXiv:2203.06142*, **2022**.
[13] A. G. Riess, A. V. Filippenko, P. Challis, A. Clocchiatti, A. Diercks, P. M. Garnavich, R. L. Gilliland, C. J. Hogan, S. Jha, R. P. Kirshner, B. Leibundgut, M. M. Phillips, D. Reiss, B. P. Schmidt, R. A. Schommer, R. Chris Smith, J. Spyromilio, C. Stubbs, N. B. Suntzeff, J. Tonry, *arXiv:2112.04510*, **2021**.
[14] K. C. Wong, S. H. Suyu, G. C.-F. Chen, C. E. Rusu, M. Millon, D. Sluse, V. Bonvin, C. D. Fassnacht, S. Taubenberger, M. W. Auger, S. Birrer, J. H. H. Chan, F. Courbin, S. Hilbert, O. Tihhonova, T. Treu, A. Agnello, X. Ding, I. Jee, E. Komatsu, A. J. Shajib, A. Sonnenfeld, R. D. Blandford, L. V. E. Koopmans, P. J. Marshall, G. Meylan, *Mon. Not. R. Astron. Soc.* **2020**, *498*, 1420.
[15] N. Aghanim, Y. Akrami, M. Ashdown, J. Aumont, C. Baccigalupi, M. Ballardini, A. J. Banday, R. B. Barreiro, N. Bartolo, S. Basak, R. Battye, K. Benabed, J.-P. Bernard, M. Bersanelli, P. Bielewicz, J. J. Bock, J. R. Bond, J. Borrill, F. R. Bouchet, F. Boulanger, M. Bucher, C. Burigana, R. C. Butler, E. Calabrese, J.-F. Cardoso, J. Carron, A. Challinor, H. C. Chiang, J. Chluba, L. P. L. Colombo, et al., *Astron. Astrophys.* **2020**, *641*, A6.
[16] D. Kirkman, D. Tytler, N. Suzuki, J. M. O'Meara, D. Lubin, *Astrophys. J. Suppl.* **2003**, *149*, 1.
[17] J. M. Shull, B. D. Smith, C. W. Danforth, *Astrophys. J.* **2012**, *759*, 23.
[18] S. D. Johnson, J. S. Mulchaey, H.-W. Chen, N. A. Wijers, T. Connor, S. Muzahid, J. Schaye, R. Cen, S. G. Carlsten, J. Charlton, M. R. Drout, A. D. Goulding, T. T. Hansen, G. L. Walths, *Astrophys. J.* **2019**, *884*, L31.
[19] T. M. C. Abbott, M. Aguena, A. Alarcon, S. Allam, O. Alves, A. Amon, F. Andrade-Oliveira, J. Annis, S. Avila, D. Bacon, E. Baxter, K. Bechtol, M. R. Becker, G. M. Bernstein, S. Bhargava, S. Birrer, J. Blazek, A. Brandao-Souza, S. L. Bridle, D. Brooks, E. Buckley-Geer, D. L. Burke, H. Camacho, A. Campos, A. Carnero Rosell, M. Carrasco Kind, J. Carretero, F. J. Castander, R. Cawthon, C. Chang, et al., *Phys. Rev. D* **2022**, *105*, 023520.
[20] C. Heymans, T. Tröster, M. Asgari, C. Blake, H. Hildebrandt, B. Joachimi, K. Kuijken, C.-A. Lin, A. G. Sánchez, J. L. van den Busch, A. H. Wright, A. Amon, M. Bilicki, J. de Jong, M. Crocce, A. Dvornik, T. Erben, M. C. Fortuna, F. Getman, B. Giblin, K. Glazebrook, H. Hoekstra, S. Joudaki, A. Kannawadi, F. Köhlinger, C. Lidman, L. Miller, N. R. Napolitano, D. Parkinson, P. Schneider, et al., *Astron. Astrophys.* **2021**, *646*, A140.
[21] R. C. Nunes, S. Vagnozzi, *Mon. Not. R. Astron. Soc.* **2021**, *505*, 5427.
[22] R. H. Becker, X. Fan, R. L. White, M. A. Strauss, V. K. Narayanan, R. H. Lupton, J. E. Gunn, J. Annis, N. A. Bahcall, J. Brinkmann, A. J. Connolly, I. Csabai, P. C. Czarapata, M. Doi, T. M. Heckman, G. S. Hennessy, Ž. Ivezic, G. R. Knapp, D. Q. Lamb, T. A. McKay, J. A. Munn, T. Nash, R. Nichol, J. R. Pier, G. T. Richards, D. P. Schneider, C. Stoughton, A. S. Szalay, A. R. Thakar, D. G. York, *Astron. J.* **2001**, *122*, 2850.
[23] M. Tegmark, A. de Oliveira-Costa, A. Hamilton, *Phys. Rev. D* **2003**, *68*, 123523.
[24] C. Gordon, W. Hu, D. Huterer, T. M. Crawford, *Phys. Rev. D* **2005**, *72*, 103002.
[25] C. J. Copi, D. Huterer, D. J. Schwarz, G. D. Starkman, *Mon. Not. R. Astron. Soc.* **2006**, *367*, 79.
[26] R. Hofmann, *Nat. Phys.* **2013**, *9*, 686.
[27] S. Hahn, R. Hofmann, D. Kramer, *Mon. Not. R. Astron. Soc.* **2019**, *482*, 4290.
[28] J. Meinert, R. Hofmann, *Universe* **2021**, *7*, 198.
[29] C.-P. Ma, E. Bertschinger, *Astrophys. J.* **1995**, *455*, 7.
[30] J. Lesgourgues, *arXiv:1104.2932*, **2011**.
[31] D. Blas, J. Lesgourgues, T. Tram, *J. Cosmol. Astropart. Phys.* **2011**, *07*, 034.
[32] M. Szopa, R. Hofmann, *J. Cosmol. Astropart. Phys.* **2008**, *03*, 001.
[33] J. Ludescher, R. Hofmann, *arXiv:0902.3898*, **2009**.
[34] Note that the information residing in the C_ℓ's is just a projection of the isotropy breaking effect since their computation assumes statistical isotropy. In Tegmark et al.,[24] Copi et al.,[26] Vielva[36] for example, statistics are considered which measure the breaking of statistical isotropy without such a projection.
[35] P. Vielva, *Adv. Astron.* **2010**, *2010*, 592094.
[36] Y. B. Zeldovich, R. A. Sunyaev, *Astrophys. Space Sci.* **1969**, *4*, 301.
[37] R. A. Sunyaev, Y. B. Zeldovich, *Comments Astrophys. Space Phys.* **1972**, *4*, 173.
[38] J. N. Bahcall, R. A. Wolf, *Astrophys. J.* **1968**, *152*, 701.
[39] G. Hurier, N. Aghanim, M. Douspis, E. Pointecouteau, *Astron. Astrophys.* **2014**, *561*, A143.
[40] P. Molaro, S. A. Levshakov, M. Dessauges-Zavadsky, S. D'Odorico, *Astron. Astrophys.* **2002**, *381*, L64.
[41] P. Noterdaeme, P. Petitjean, R. Srianand, C. Ledoux, S. López, *Astron. Astrophys.* **2011**, *526*, L7.
[42] P. Noterdaeme, J. -K. Krogager, S. Balashev, J. Ge, N. Gupta, T. Krühler, C. Ledoux, M. T. Murphy, I. Pâris, P. Petitjean, H. Rahmani, R. Srianand, W. Ubachs, *Astron. Astrophys.* **2017**, *597*, A82.
[43] A. Songaila, L. L. Cowie, S. Vogt, M. Keane, A. M. Wolfei, E. M. Hu, A. L. Oren, D.-R. Tytleri, K. M. Lanzetta, *Nature* **1994**, *371*, 43.
[44] J. Ge, J. Bechtold, J. H. Black, *Astrophys. J.* **1997**, *474*, 67.
[45] R. Srianand, P. Petitjean, C. Ledoux, *Nature* **2000**, *408*, 931.
[46] S. Muller, A. Beelen, J. H. Black, S. J. Curran, C. Horellou, S. Aalto, F. Combes, M. Guélin, C. Henkel, *Astron. Astrophys.* **2013**, *551*, A109.

[47] D. A. Riechers, A. Weiss, F. Walter, C. L. Carilli, P. Cox, R. Decarli, R. Neri, *Nature* **2022**, *602*, 58.
[48] K. C. Roth, D. M. Meyer, I. Hawkins, *Astrophys. J.* **1993**, *413*, L67.
[49] J. C. Mather, E. S. Cheng, D. A. Cottingham, R. E. Eplee, Jr., D. J. Fixsen, T. Hewagama, R. B. Isaacman, K. A. Jensen, S. S. Meyer, P. D. Noerdlinger, S. M. Read, L. P. Rosen, R. A. Shafer, E. L. Wright, C. L. Bennett, N. W. Boggess, M. G. Hauser, T. Kelsall, S. H. Moseley, Jr., R. F. Silverberg, *Astrophys. J.* **1994**, *420*, 439.
[50] To a very good approximation Mather et al.[50] the spectral intensity $I(\nu)$ of today's CMB is given as $I_{z=0}(\nu) = 16\pi^2 \frac{\nu^3}{\exp(\frac{2\pi\nu}{T(z=0)})-1}$. If we assume a TRR of $T(z=0) = \frac{1}{f(z)} T(z)$ and a FRR of $\nu(z=0) = \frac{1}{g(z)}\nu'$ with $f(z) \neq g(z)$ then the Stefan– Boltzmann law still is redshifted according to the TRR: $\int \mathrm{d}\nu I_{z=0}(\nu) = \frac{\pi^2}{15} T^4(z=0) = \frac{\pi^2}{15} (\frac{T(z)}{f(z)})^4 = (\frac{1}{g(z)})^4 \int \mathrm{d}\nu' I_z(\nu')$ where $\mathrm{d}\nu' I_z(\nu') = \mathrm{d}\nu' 16\pi^2 \frac{(\nu')^3}{\exp(\frac{f(z)}{g(z)} \frac{2\pi\nu'}{T(z)})-1}$. However, the maximum $\nu_{\max} = \frac{2.821}{2\pi} T(z=0)$ of the distribution $\mathrm{d}\nu I_{z=0}(\nu)$ converts to a maximum $\nu'_{\max} = \frac{2.821}{2\pi} \frac{g(z)}{f(z)} T(z)$ of the distribution $\mathrm{d}\nu' I_z(\nu')$. Thus, $I_z(\nu')$ would not be a blackbody spectrum for $g(z) \neq f(z)$.
[51] R. Hofmann, J. Meinert, **2023**.
[52] J. C. Mather, E. S. Cheng, R. E. Eplee, Jr., R. B. Isaacman, S. S. Meyer, R. A. Shafer, R. Weiss, E. L. Wright, C. L. Bennett, N. W. Boggess, E. Dwek, S. Gulkis, M. G. Hauser, M. Janssen, T. Kelsall, P. M. Lubin, S. H. Moseley, Jr., T. L. Murdock, R. F. Silverberg, G. F. Smoot, *Astrophys. J. Lett.* **1990**, *354*, L37.
[53] S. Hahn, R. Hofmann, *Mod. Phys. Lett. A* **2018**, *2016*, 1850029.
[54] Two polarisations for the massless mode, three polarisations for each of the two massive modes.
[55] R. Hofmann, *Ann. Phys.* **2015**, *527*, 254.
[56] P. A. R. Ade, N. Aghanim, M. Arnaud, M. Ashdown, J. Aumont, C. Baccigalupi, A. J. Banday, R. B. Barreiro, J. G. Bartlett, N. Bartolo, E. Battaner, R. Battye, K. Benabed, A. Benoît, A. Benoit-Lévy, J.-P. Bernard, M. Bersanelli, P. Bielewicz, J. J. Bock, A. Bonaldi, L. Bonavera, J. R. Bond, J. Borrill, F. R. Bouchet, F. Boulanger, M. Bucher, C. Burigana, R. C. Butler, E. Calabrese, J.-F. Cardoso, et al., *Astron. Astrophys.* **2016**, *594*, A13.
[57] The success of ΛCDM as a low-z model is suggested by the agreement of its parameter values when extracted from purely local and different cosmology probes, see Abdalla et al.[13]
[58] F. Giacosa, R. Hofmann, M. Neubert, *J. High Energy Phys.* **2008**, *02*, 077.
[59] R. Hofmann, *AIP Conf. Proc.* **2018**, *1978*, 300006.
[60] R. Hofmann, T. Grandou, *Universe* **2022**, *8*, 117.
[61] S. L. Adler, W. A. Bardeen, *Phys. Rev.* **1969**, *182*, 1517.
[62] S. L. Adler, *Phys. Rev.* **1969**, *177*, 2426.
[63] J. Bell, R. Jackiw, *Nuovo Cimento A* **1969**, *60*, 47.
[64] K. Fujikawa, *Phys. Rev. Lett.* **1979**, *42*, 1195.
[65] K. Fujikawa, *Phys. Rev. D* **1980**, *21*, 2848.
[66] S.-J. Sin, *Phys. Rev. D* **1994**, *50*, 3650.
[67] S. U. Ji, S. J. Sin, *Phys. Rev. D* **1994**, *50*, 3655.
[68] T. Matos, F. S. Guzman, *Classical Quantum Gravity* **2000**, *17*, L9.
[69] H.-Y. Schive, T. Chiueh, T. Broadhurst, *Nat. Phys.* **2014**, *10*, 496.
[70] J. C. Niemeyer, *Prog. Part. Nucl. Phys.* **2020**, *113*, 103787.
[71] N. Aghanim, M. Arnaud, M. Ashdown, J. Aumont, C. Baccigalupi, A. J. Banday, R. B. Barreiro, J. G. Bartlett, N. Bartolo, E. Battaner, K. Benabed, A. Benoît, A. Benoit-Lévy, J.-P. Bernard, M. Bersanelli, P. Bielewicz, J. J. Bock, A. Bonaldi, L. Bonavera, J. R. Bond, J. Borrill, F. R. Bouchet, F. Boulanger, M. Bucher, C. Burigana, R. C. Butler, E. Calabrese, J.-F. Cardoso, A. Catalano, A. Challinor, et al., *Astron. Astrophys.* **2016**, *594*, A11.
[72] M. Schwarz, R. Hofmann, F. Giacosa, *J. High Energy Phys.* **2007**, *02*, 091.
[73] G. Hinshaw, A. J. Banday, C. L. Bennett, K. M. Gorski, A. Kogut, C. H. Lineweaver, G. F. Smoot, E. L. Wright, *Astrophys. J. Lett.* **1996**, *464*, L25.
[74] C. J. Copi, D. Huterer, D. J. Schwarz, G. D. Starkman, *Phys. Rev. D* **2007**, *75*, 023507.
[75] C. J. Copi, D. Huterer, D. J. Schwarz, G. D. Starkman, *Mon. Not. R. Astron. Soc.* **2015**, *451*, 2978.
[76] C. J. Copi, D. Huterer, D. J. Schwarz, G. D. Starkman, *Mon. Not. R. Astron. Soc.* **2011**, *418*, 505.
[77] H. K. Eriksen, F. K. Hansen, A. J. Banday, K. M. Gorski, P. B. Lilje, *Astrophys. J.* **2004**, *605*, 14.
[78] Y. Akrami, M. Ashdown, J. Aumont, C. Baccigalupi, M. Ballardini, A. J. Banday, R. B. Barreiro, N. Bartolo, S. Basak, K. Benabed, M. Bersanelli, P. Bielewicz, J. J. Bock, J. R. Bond, J. Borrill, F. R. Bouchet, F. Boulanger, M. Bucher, C. Burigana, R. C. Butler, E. Calabrese, J.-F. Cardoso, B. Casaponsa, H. C. Chiang, L. P. L. Colombo, C. Combet, D. Contreras, B. P. Crill, P. de Bernardis, G. de Zotti, et al., *Astron. Astrophys.* **2020**, *641*, A7.
[79] A. de Oliveira-Costa, M. Tegmark, M. Zaldarriaga, A. Hamilton, *Phys. Rev. D* **2004**, *69*, 063516.
[80] C. J. Copi, D. Huterer, D. J. Schwarz, G. D. Starkman, *Mon. Not. R. Astron. Soc.* **2015a**, *449*, 3458.
[81] A. Notari, M. Quartin, *J. Cosmol. Astropart. Phys.* **2015**, *06*, 047.
[82] D. J. Schwarz, C. J. Copi, D. Huterer, G. D. Starkman, *Classical Quantum Gravity* **2016**, *33*, 184001.
[83] J. Kim, P. Naselsky, *Astrophys. J. Lett.* **2010**, *714*, L265.
[84] P. K. Aluri, P. Jain, *Mon. Not. R. Astron. Soc.* **2012**, *419*, 3378.
[85] A. Gruppuso, N. Kitazawa, M. Lattanzi, N. Mandolesi, P. Natoli, A. Sagnotti, *Phys. Dark Universe* **2018**, *20*, 49.
[86] P. Fosalba, E. Gaztañaga, *Mon. Not. R. Astron. Soc.* **2021**, *504*, 5840.
[87] S. Yeung, M.-C. Chu, *Phys. Rev. D* **2022**, *105*.
[88] P. Vielva, E. Martinez-Gonzalez, R. B. Barreiro, J. L. Sanz, L. Cayon, *Astrophys. J.* **2004**, *609*, 22.
[89] M. Cruz, E. Martinez-Gonzalez, P. Vielva, in Highlights of Spanish Astrophysics V (Eds: J. Diego, L. Goicoechea, J. Gonzz-Serrano, J. Gorgas), *Astrophysics and Space Science Proceedings*, Springer, Berlin **2010**, p. 275.
[90] S. Hahn, R. Hofmann, *Mon. Not. R. Astron. Soc.* **2017**, *469*, 1233.
[91] R. Hofmann, *arXiv:0710.1169*, **2007**.
[92] C. Falquez, R. Hofmann, T. Baumbach, *Ann. Phys.* **2010**, *522*, 904.
[93] M. Schwarz, R. Hofmann, F. Giacosa, *Int. J. Mod. Phys. A* **2007b**, *22*, 1213.
[94] J. Lesgourgues, T. Tram, *J. Cosmol. Astropart. Phys.* **2011**, *09*, 032.
[95] Even though the dependences of $\epsilon(q,a)$ and $G(q,a)$ on scale factor a and redshift z are different, we abuse notation by writing $\epsilon(q,z)$ and $G(q,z)$.
[96] U. Seljak, M. Zaldarriaga, *Astrophys. J.* **1996**, *469*, 437.
[97] M. Doran, *J. Cosmol. Astropart. Phys.* **2005**, *2005*, 011.
[98] A. Lewis, A. Challinor, A. Lasenby, *Astrophys. J.* **2000**, *538*, 473.
[99] Matching at z_{match} means that for $z \geq z_{\text{match}}$ we set $G \equiv 0$ in the Boltzmann hierarchy while G is taken from a precomputed table for $z < z_{\text{match}}$.